

Quantitative ferroelectric characterization of single submicron grains in Bi-layered perovskite thin films

C. Harnagea, A. Pignolet, M. Alexe, D. Hesse, U. Gösele

Max-Planck-Institut für Mikrostrukturphysik, Weinberg 2, D-06120 Halle (Saale), Germany
(Fax: +49-345/5511-223, E-mail: charna@mpi-halle.mpg.de)

Received: 13 July 1999/Accepted: 5 October 1999/Published online: 23 February 2000 – © Springer-Verlag 2000

Abstract. The local polarization state and the electromechanical properties of ferroelectric thin films can be probed via the converse piezoelectric effect using scanning force microscopy (SFM) combined with a lock-in technique. This method, denominated as piezoresponse SFM, was used to characterize at the nanoscale level ferroelectric $\text{SrBi}_2\text{Ta}_2\text{O}_9$ and $\text{Bi}_4\text{Ti}_3\text{O}_{12}$ thin films, grown by pulsed laser deposition. Two types of samples were studied: polycrystalline films, with grains having random orientations, and epitaxial films, consisting of (100)_{orth}- or (110)_{orth}-oriented crystallites, 100 nm to 2 μm in lateral size, which are embedded into a (001)-oriented matrix. The ferroelectric domain structure was imaged and the piezoelectric response under different external conditions was locally measured for each type of sample. Different investigation procedures are described in order to study the ferroelectric properties via the electromechanical response. A distinct ferroelectric behavior was found for single grains of $\text{SrBi}_2\text{Ta}_2\text{O}_9$ as small as 200 nm in lateral size, as well as for 1.2 $\mu\text{m} \times 175$ nm crystallites of $\text{Bi}_4\text{Ti}_3\text{O}_{12}$. By probing separately the crystallites and the matrix the investigations have demonstrated *at the nanoscale level* that $\text{SrBi}_2\text{Ta}_2\text{O}_9$ has no spontaneous polarization along its crystallographic *c*-axis, whereas $\text{Bi}_4\text{Ti}_3\text{O}_{12}$ exhibits a piezoelectric behavior along both the *a*- and *c*-directions. The electrostriction coefficients were estimated to be $3 \times 10^{-2} \text{ m}^4/\text{C}^2$ for polycrystalline $\text{SrBi}_2\text{Ta}_2\text{O}_9$ and $7.7 \times 10^{-3} \text{ m}^4/\text{C}^2$ for *c*-oriented $\text{Bi}_4\text{Ti}_3\text{O}_{12}$.

Quantitative measurements at the nanoscale level, within the experimental errors give the same values for remanent polarization and coercive field as macroscopic ferroelectric measurements performed on the same samples.

PACS: 07.79.-v; 77.80.Dj; 77.65.Bn

an appropriate description of the basic local processes in ferroelectric thin films. Therefore, it is of both fundamental and practical interest to investigate whether ferroelectric structures with nanometer sizes still exhibit ferroelectric, piezoelectric, and pyroelectric properties, as well as to study how these properties are affected by the size [1]. Although the macroscopic dielectric, piezoelectric, and ferroelectric characteristics of perovskite-type ferroelectrics (especially the PZT family and the Bi-oxide layered perovskite compounds) have intensively been investigated [2, 3], only a few experimental data on their properties measured at the nm scale are available. Among several electric scanning force microscopy (SFM) techniques [4] the piezoresponse mode of SFM has proven to be the most suitable method to study and to *control* the ferroelectric domain structure at the nm scale. This technique was first used by Gütthner and Dransfeld [5] to polarize and image thin copolymer films at the μm scale. The characterization of domain reversal in lead zirconate titanate (PZT) films by recording *local hysteresis loops* was first reported by Hidaka et al. [6]. Systematic studies of domain dynamics, retention, and fatigue effects have already been reported for thin films of PZT-based materials [7, 8]. However, the first results concerning the observation of the ferroelectric domain structure of $\text{SrBi}_2\text{Ta}_2\text{O}_9$ (SBT) thin films were only reported in 1998 [9].

This paper demonstrates that the piezoresponse SFM method represents a powerful tool not only for imaging the ferroelectric domain structure, but also to perform local quantitative measurements on ferroelectric thin films. It is shown that the local piezoelectric constant, the polarization, and the electrostriction coefficient can be estimated using the piezoelectric response of the sample. Measurements on SBT and $\text{Bi}_4\text{Ti}_3\text{O}_{12}$ (BiT) thin films revealed piezoelectric coefficients of 2 pm/V and 8 pm/V, respectively, under the poling voltages applied. The electrostriction coefficients calculated were $0.03 \text{ m}^4/\text{C}^2$ for SBT and $7.7 \times 10^{-3} \text{ m}^4/\text{C}^2$ for *c*-oriented BiT. Ferroelectric domain visualization in BiT thin films is reported for the first time and it is proved that a single crystallite of SBT with only 200 nm lateral size exhibits ferroelectric properties.

Ferroelectric thin films are very attractive in view of their possible applications in nonvolatile memories, microelectromechanical devices, and pyroelectric detectors. The decrease in size (down to tens of nm) of microelectronic devices requires

1 Experimental

1.1 The piezoresponse SFM method

This technique is based on the detection of local vibrations of a ferroelectric sample induced by a testing ac signal applied between the conductive tip of the SFM and the bottom electrode of the sample. The mechanical oscillations of the sample underneath the tip modulate the global deflection signal and are detected using a lock-in technique. Because the first harmonic of the oscillations represents the piezoelectric constant, it is further referred to as *piezoresponse* signal [10].

The piezoelectric constant d_{33} of a given point can be determined as follows:

$$v_{\omega} = \delta d_{33} A_{\omega}, \quad (1)$$

where v_{ω} is the amplitude of the piezoresponse signal, A_{ω} the amplitude of the testing ac voltage, and δ the sensitivity of the optical detector, which is in fact the conversion factor between the mechanical displacement of the SFM tip and the electric deflection signal.

It is well known that for ferroelectric materials with a centrosymmetric paraelectric phase the piezoelectric effect can be considered as the electrostriction effect biased by the spontaneous polarization P [11]:

$$d_{33} = 2Q\varepsilon_{33}P. \quad (2)$$

Therefore, for these ferroelectric materials the piezoresponse signal image represents in fact an image of the ferroelectric domain pattern. Moreover, the absolute value of the polarization can be estimated if the electrostriction coefficient Q and the dielectric constant ε_{33} are known.

It is important to note that for imaging the ferroelectric domain pattern without modifying it, the testing ac voltage has to be as low as possible. Under an ac voltage higher than the local coercive voltage, switching of polarization occurs, modifying the actual domain pattern. However, to enhance the signal-to-noise ratio, the testing voltage has to be as high as possible in order to get a high amplitude of the mechanical vibration and thus, according to (1), a high piezoresponse signal. The main noise source during the acquisition of the piezoresponse images is the global deflection signal itself, from which the first-harmonic signal is extracted. The deflection signal, which is used by the SFM system as a feedback to maintain a constant force between tip and sample, is proportional to the scanning speed and to the derivative of the surface height with respect to the scan direction. For samples with a high roughness, the deflection signal exhibits very sharp high peaks. These fast variations of the deflection signal may have harmonic components with the same frequency as the ac testing voltage and amplitudes comparable with the piezoresponse signal. This noise may be overcome by using a low scanning speed and a high-frequency probing voltage. However, this leads to a long recording time necessary for the acquisition of the image.

Another important parameter governing the piezoresponse imaging of ferroelectric domains is the contact force between the conductive tip and the surface of the sample. Zavala et al. [12] reported a 30% decrease of the piezoelectric constant of undoped PZT while increasing the contact force from 10 μN to 23 μN . Similarly, Gruverman and

Ykeda [9] could increase the piezoresponse signal by 30% for SBT samples by using a very low contact force (of 1 nN) between tip and sample. However, measurements on non-ferroelectric samples carried out by Christman et al. [13] showed that the effect of the electrostatic interaction between tip/cantilever and sample/bottom electrode on the first-harmonic signal is significant for soft cantilevers with a force constant $< 0.3 \text{ N/m}$. Therefore, in order to minimize the electrostatic interaction, a high spring constant of the cantilever may be required, even if this implies the use of a high contact force between tip and sample.

1.2 Local quantitative measurements

The SFM conductive tip represents in fact a nanometer-sized movable top electrode used for probing the sample surface by applying an ac voltage. This top electrode can be fixed over any desired place of the sample surface, in order to explore only that area. Taking into account that the sample is tested by detecting the induced oscillations, several procedures can be used to measure the local properties.

1.2.1 Amplitude sweep. The local piezoelectric constant can be determined with a high accuracy by sweeping the amplitude of the testing ac voltage from zero up to the local coercive voltage of the sample. The piezoelectric constant can be easily calculated from the slope of the linear dependence expressed in (1). In the case of ferroelectrics, as soon as the ac amplitude is higher than the local coercive voltage, the polarization starts to switch with the same frequency leading to a decrease of the first harmonic response.

1.2.2 Piezoelectric constant versus stress dependence. The influence of the mechanical stress on the piezoelectric constant can be studied by varying the contact force between the tip and sample while recording the piezoresponse signal. In general, the piezoelectric constant decreases when the stress increases.

1.2.3 Hysteresis loops. The most important characterization and also an incontestable proof of ferroelectricity is the presence of piezoelectric hysteresis. This measurement is generally performed using a dc bias source connected in series with the ac voltage source. The hysteresis loops are obtained by sweeping the bias voltage and recording the piezoresponse signal. There are two main procedures that may be used:

In the first procedure, the probing ac voltage is superimposed on the dc bias which is varied in steps from zero to V_{max} , then decreased down to V_{min} and increased again up to V_{max} , in order to measure the piezoelectric constant as a function of the field applied *simultaneously*. Each step of the bias has a duration t_{bias} . The loop obtained in this manner is further referred to as *in-field* hysteresis loop and represents a normal $d - E$ curve [15], as it is often used for the characterization of the macroscopic piezoelectric properties of thin films.

In the second procedure, the dc bias voltages are in fact pulses with a duration t_{bias} . After a time interval t_{delay} from the suppression of the polarizing pulse, the piezoresponse signal is recorded and stored [6, 13]. The amplitudes of the pulses are varied in steps in the same way as in the first procedure. Using this measuring method, the electrostatic interactions

between tip/cantilever and the bottom electrode are avoided during the measurement and only the *remanent* piezoelectric coefficient is measured as a function of the dc voltage pulse *previously* applied to the sample. The loop obtained accordingly is further referred to as *remanent* hysteresis loop. This kind of measurement also reveals the retention characteristics of ferroelectric thin films.

Whereas the remanent loop is saturated for high values of the poling voltage, the in-field loop contains a linear part. It was found that if this linear component is subtracted, the obtained curve nearly coincides with the remanent hysteresis loop.

It may be speculated that the electrostatic interaction between the tip/cantilever and bottom electrode is responsible for the linear component of the first-harmonic signal which modulates the first-harmonic signal as explained by Christman et al. [13]. This is not the case here, due to the high elastic constant used for the cantilever, about 20 times higher than the value over which the effect of this interaction became insignificant in their experiments. Moreover, the analysis performed by Franke [15], revealed that the component of the first-harmonic signal due to the Maxwell stress should be shifted in phase by 180° with respect to the piezoresponse signal. This leads to the conclusion that, if the electrostatic interaction would be present in the first harmonic with a linear component, then the slope of this component would be negative.

1.2.4 Measurement of the electrostriction coefficient. The linear part of the in-field loop is due to a real increase of the piezoelectric constant and can be used to estimate the local electrostriction coefficient Q . Relation (2) can be written as (3), by considering the total polarization P of the poled volume.

$$d_{33} = 2Q\varepsilon_{33}(P + \varepsilon_{33}E). \quad (3)$$

The slope of the linear component can be obtained by differentiating (3) with respect to E , for those regions where the ferroelectric polarization $P = \text{const.}$, i.e. at the saturation:

$$\frac{\partial d_{33}}{\partial E} = 2Q\varepsilon_{33}^2. \quad (4)$$

The electrostriction coefficient can be estimated if the permittivity is known from other measurements.

1.3 Experimental setup

The experimental setup is very similar to the one used by other authors [10, 16]. A commercial scanning probe microscope (Dimension 5000, Digital Instruments) working in contact mode was adapted to measure the vibrations of the sample surface. The small mechanical oscillations are detected from the global deflection signal using a lock-in amplifier (EG&G Instruments, Model 7260).

The probing ac signal had a frequency $f = 16.7$ kHz and an amplitude $A_\omega = 2.1$ V. This amplitude proved to be low enough not to influence the domain structure. The dc bias voltage source, the ac source, and the lock-in amplifier were all controlled by a computer, using an adequate software. The voltages applied to the sample for hysteresis measurements

had the following parameters: $t_{\text{bias}} = 500$ ms for the in-field loops; $t_{\text{bias}} = 100$ ms and $t_{\text{delay}} = 2$ s for the remanent loops. The number of steps between V_{min} and V_{max} was usually set to 100.

The voltages were applied to the sample using highly doped silicon cantilevers, with a resistivity of $0.02 \Omega \text{ cm}$, a resonance frequency of 334 kHz, and a spring constant of 38 N/m. The experiments presented here were carried out using contact forces between $0.2 \mu\text{N}$ and $1.7 \mu\text{N}$. The radius of the tip apex was estimated to be about 30 nm, a value which represents the lower limit for the lateral resolution achieved.

2 Results and discussions

Ferroelectric SBT and BiT thin films were grown on 150-nm-thick LaNiO_3 (LNO) epitaxial electrode layers which were grown onto epitaxial CeO_2/YSZ buffer layers on Si(100) wafers (YSZ – yttria-stabilized zirconia). The intermediate layers between the ferroelectric film and the substrate serve as a template for epitaxial growth. The 150-nm-thick epitaxial LNO layer also serves as a bottom electrode. All films were grown by pulsed laser deposition at elevated substrate temperatures. Details on deposition conditions, morphology and macroscopic ferroelectric properties can be found elsewhere [17–19].

Piezoresponse SFM was used to characterize two types of SBT and BiT samples: (i) polycrystalline and (ii) epitaxial films with isolated crystallites embedded in a flat matrix.

2.1 Characterization of grains in polycrystalline films

The SBT films consist of grains having lateral sizes of the order of 200 nm and heights of about 50 nm. Figure 1a and 1b show the surface morphology and the ferroelectric domain structure, respectively. White and black regions in the piezoresponse image correspond to positive (polarization upward) and negative ferroelectric domains, respectively. The regions without a net black or white contrast correspond to areas of the sample that possess a very weak piezoelectric activity. This fact was discussed in [9] and it was concluded that it is due mainly to the domains having randomly oriented polarization. As it can be noticed by comparing the topography and the domain structure of the region, this conclusion is verified: the gray regions in the piezoresponse image correspond to single grains in the topographic image. The ratio of

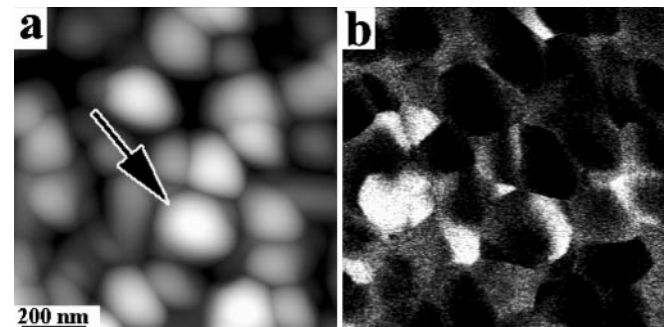


Fig. 1a,b. Simultaneously obtained topographic (a) and piezoresponse (b) images of a SBT film

the surface area having a high piezoresponse signal is about 30%, measured over $5 \times 5 \mu\text{m}$. The grain indicated by an arrow in Fig. 1a was chosen for further characterization. This grain has an initial domain structure, i.e. it is divided into two opposite domains as it can be seen in the piezoresponse image (Fig. 1b). The experiments are illustrated in Figs. 2 and 3. The contour lines in Fig. 2a designate the area of the mechanical interaction between the SFM tip and the surface of the grain. Due to the tip–grain geometry, this contour does not exactly coincide with the shape of the grain. In Fig. 3a, the in-field and the remanent hysteresis loops are shown.

The slope of the linear part of the in-field hysteresis loop in Fig. 3a was found to be $0.2 \pm 0.05 \text{ pm/V}^2$. By considering a thickness of the sample of 200 nm, as revealed by cross-section TEM analysis (not shown here), and $\epsilon_{33} = 100\epsilon_0$, as measured from macroscopic measurements, a value $Q = 0.03 \pm 0.01 \text{ m}^4/\text{C}^2$ was found for the electrostriction coefficient. This value is about 3 times lower than that measured by Kholkin et al. [20] on polycrystalline SBT films. The remanent polarization was estimated using (2). From the value of $d_{33} = 2 \text{ pm/V}$ (from the piezoelectric hysteresis loop) for the remanent polarization the value $P = 3.7 \mu\text{C}/\text{cm}^2$ was derived. Using a RT66A ferroelectric tester, the macroscopic remanent polarization for the same sample was found to be $1 \mu\text{C}/\text{cm}^2$. This value represents 27% from the value estimated by piezoresponse SFM, which very closely relates to the ratio of the film area that has a strong piezoelectric signal. For comparison, the nanoscopic in-field polarization hysteresis loop and the macroscopic one are shown in Fig. 3b.

Figures 2c and 2d show the topography and the domain structure of the grain after the hysteresis measurements. The last voltage applied was $+V_{\text{max}} = 20 \text{ V}$, therefore the polar-

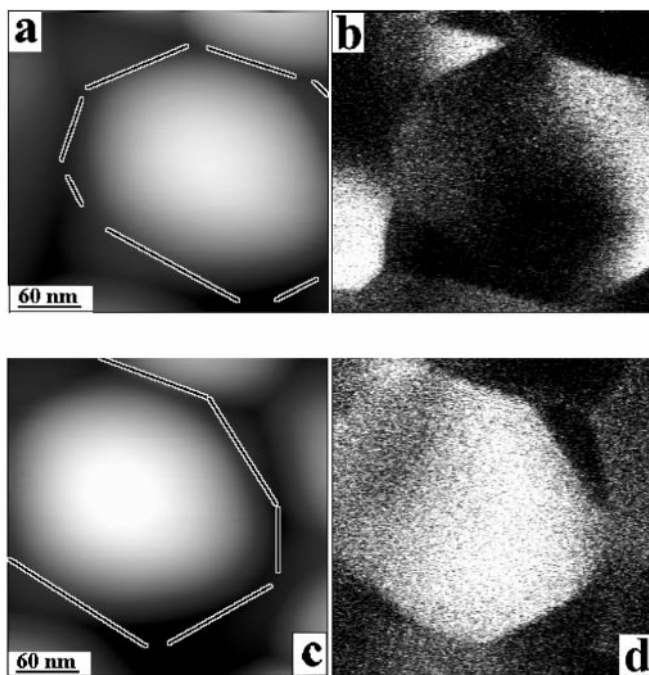


Fig. 2. a Topography and b initial domain structure of a SBT grain; c topographic and d piezoresponse images of the grain after applying a positive dc voltage

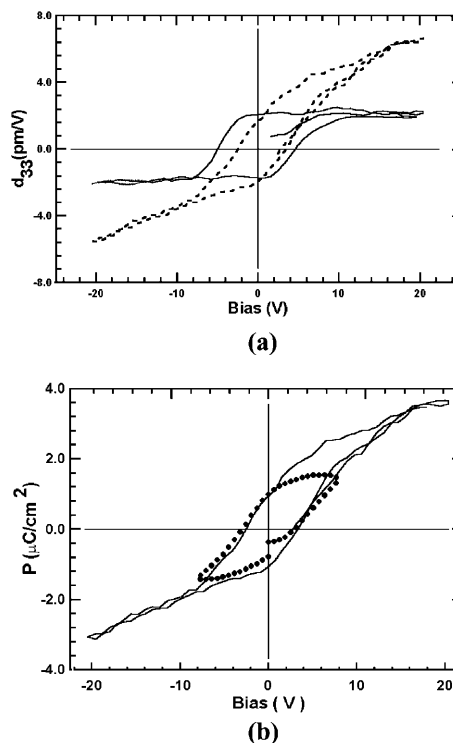


Fig. 3. a Comparison between the remanent (–) and in-field (●) hysteresis loops obtained on a SBT film at the point indicated in Fig. 2c. b Estimated polarization for the in-field hysteresis loop (–) obtained by piezoresponse SFM compared with the macroscopic polarization hysteresis loop (●) measured with a standard ferroelectric tester on the same sample

ization state remained positive, which is demonstrated by the white contrast of the entire grain.

The dependence of the piezoelectric constant on the contact force is shown in Fig. 4. When the loading force increased from 200 nN to 1600 nN, the piezoelectric constant decreased by about 50%. This is generally considered an effect of the mechanical clamping of the film under an applied stress. Most probably, the very low value measured for the piezoelectric coefficient is determined by the very high contact force used.

The same experiments were performed on a BiT ferroelectric thin film. Figure 5a shows the morphology of the film, which consists of grains of about 300 nm in lateral size. The arrow indicates the grain that was subjected to measurements. The initial ferroelectric polarization state of the grain is nega-

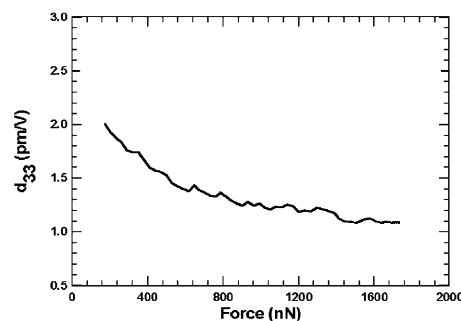


Fig. 4. Dependence of the local piezoelectric constant of a SBT grain on the contact force between the tip and the surface

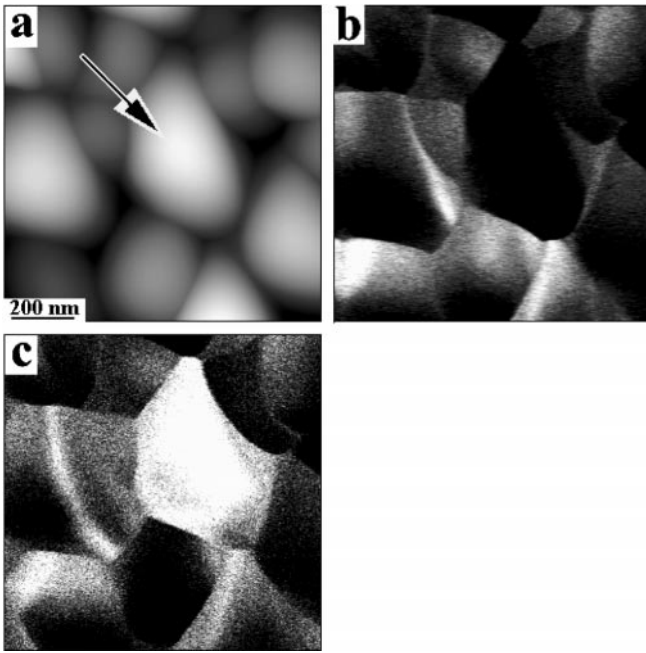


Fig. 5. **a** Topographic image of a BiT ferroelectric film. **b, c** Piezoresponse images of the same area before (**b**) and after (**c**) performing the hysteresis loop measurement at the point marked by an arrow in **a**

tive as shown in Fig. 5b. The piezoelectric hysteresis loops shown in Fig. 6a were taken at the point marked by the arrow in Fig. 5a. The remanent piezoelectric hysteresis loop shows a significant decrease of the piezoelectric constant at high values of the applied pulses. The decrease of the piezoelectric constant in ferroelectric materials at high electric fields

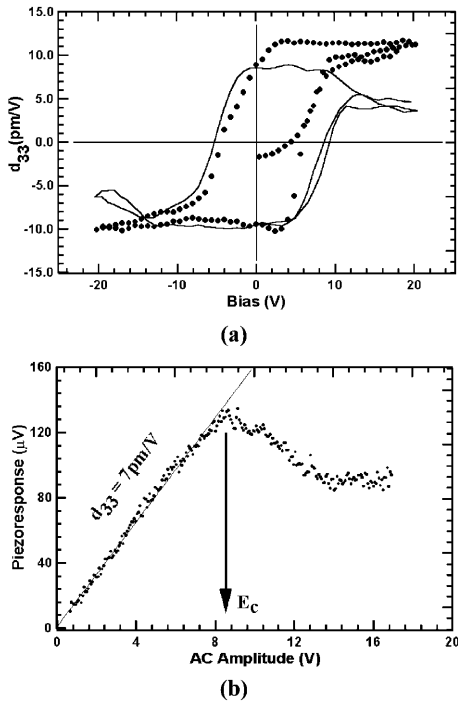


Fig. 6. **a** Remanent (—) and in-field (•) hysteresis loops of the grain shown in Fig. 5. **b** Dependence of the piezoresponse signal on the amplitude of the ac signal

has been seen before on macroscopic measurements [21, 22] and is considered an effect of the variation of the permittivity in relation (2). As it is well known, the dielectric constant decreases with the applied electric field and this may generally cause a decrease of d_{33} according to (2). However, this is not the case here, since the measuring procedure was that of the remanent hysteresis loop, i.e. without any bias applied during the measurement of the piezoelectric constant. This effect should rather appear in the in-field hysteresis loop and not in the remanent one. The stress-induced depolarization, recently reported by Franke et al. [23] for PZT thin films, may be the origin of this effect. Further experiments are in progress to elucidate this effect. In Fig. 6b the dependence of the piezoresponse signal on the amplitude of the ac voltage is shown. According to (1), the slope of the curve represents the piezoelectric coefficient, measured with a better accuracy. In this case, the value of 7 pm/V was found after poling the area underneath the tip with a dc bias of 20 V. Above 8 V amplitude, which corresponds well to the coercive field of the remanent loop (Fig. 6a), the piezoresponse signal decreases, indicating the polarization switching.

Experiments carried out to study the effect of the contact force on the piezoelectric coefficient did not reveal any dependence up to 1700 nN for the BiT film.

2.2 Characterization of individual grains within epitaxial films

A second set of experiments was performed on epitaxial SBT and BiT films each of them consisting of a very flat c -oriented matrix in which $(100)_{\text{orth}}$ - and $(110)_{\text{orth}}$ -oriented crystallites are embedded [19]. These crystallites having lateral sizes from 100 nm up to 1–2 μm are square or rectangular in shape.

Figures 7 and 8 show the results of the experiments performed on an epitaxial SBT ferroelectric thin film. The 190 nm \times 270 nm crystallite protruding 20 nm out of the surface shown in the topographic image (Fig. 7a) appears in the

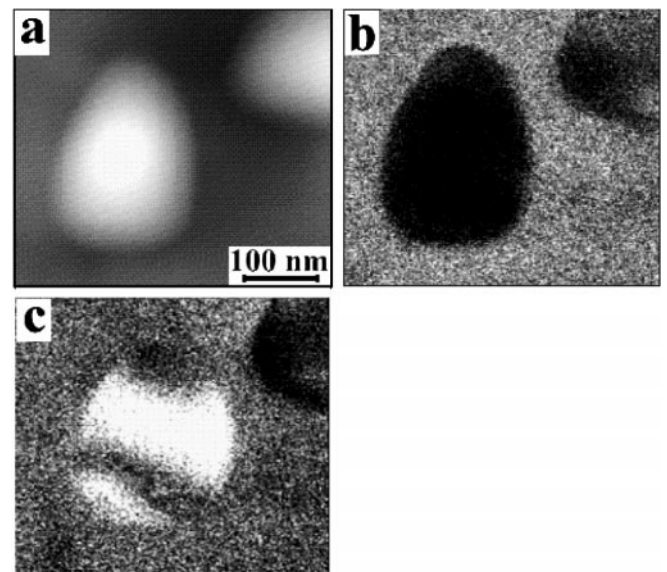


Fig. 7. **a** Topographic image of a SBT epitaxial film showing a $(110)_{\text{orth}}$ -oriented grain embedded in the c -oriented background. **b** Piezoresponse image of the grain, showing the initial domain structure. **c** Ferroelectric domain structure of the grain, after applying a +12 V dc pulse

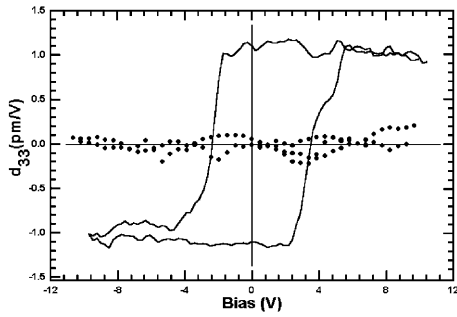


Fig. 8. Remanent piezoelectric hysteresis loops of the crystallite (—) shown in Fig. 7 and of the c -oriented background (●)

corresponding piezoresponse image (Fig. 7b) with a negative initial polarization. Most of the grains have initially the polarization vector oriented towards the bottom electrode, probably due to the asymmetry of the heterostructure. The surroundings of the grain, i.e. the c -oriented matrix, do not exhibit a piezoelectric activity, within the noise limit of the system. A poling experiment (not shown here) performed over an area of $5\ \mu\text{m} \times 5\ \mu\text{m}$ by scanning the tip while a dc voltage of $+15\ \text{V}$ was applied to the bottom electrode produced the change in contrast only for the embedded grains, the flat background remaining unchanged. To further demonstrate the absence of the spontaneous polarization along the c axis of the SBT unit cell, the remanent hysteresis loops acquired with the tip fixed on top of the grain (in the middle) and over a point of the matrix, respectively, are presented in Fig. 8. These curves clearly demonstrate the presence of spontaneous polarization only for the protruding crystallites, i.e. normal to $(100)_{\text{orth}}$ or $(110)_{\text{orth}}$ crystallographic planes [19].

It is known that a fundamental issue in today's physics of the ferroelectric memories is to find out the lowest dimension of a ferroelectric capacitor still exhibiting ferroelectric properties [24]. The well-rectangular-shaped hysteresis loop of the grain represents an incontestable proof that a SBT structure 200 nm in lateral size and 150 nm thick is still ferroelectric. The switching of the grain is proved by the piezoresponse image shown in Fig. 7c, acquired after the last voltage applied to the grain was 10 V. The grain possesses a distinct thin ferroelectric domain structure, with lateral sizes of the domains down to 40 nm, and with positive and negative domains alternating over the grain length.

Switching and local characterization of $(110)_{\text{orth}}$ -oriented grains of BiT embedded into the c -oriented matrix are presented in Figs. 9 and 10. The topographic image Fig. 9a shows a flat background from which a needle-shaped grain of $1.2\ \mu\text{m} \times 175\ \text{nm}$ is protruding out by about 30 nm. Cross-section TEM analysis revealed that the crystallites are extending into depth by about 365 nm within the c -oriented matrix of 500 nm thickness. The corresponding piezoresponse image, Fig. 9b, indicates that the initial polarization state is negative while the matrix does not show a piezoelectric activity. The SFM conductive tip was fixed at the point marked by the cross (Fig. 9a) in order to perform the local characterization. The results are presented in Fig. 10a. The remanent hysteresis loop exhibits a stronger effect of depolarization at high field than in the case of polycrystalline BiT. The maximum value of $d_{33} = 4\ \text{pm/V}$ is about two times smaller. However, the switching of this crystallite is clearly shown in

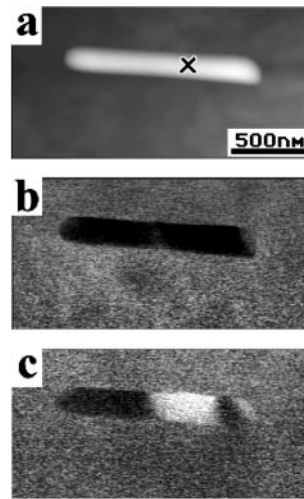


Fig. 9. **a** Topography of a $(110)_{\text{orth}}$ -oriented crystallite of BiT embedded in the c -oriented background. **b** Piezoresponse image showing the initial domain structure of the grain. **c** The ferroelectric domain structure of the crystallite after decreasing the voltage applied from $V_{\text{max}} = +30\ \text{V}$ to zero

Fig. 9c, acquired after the poling voltage was reduced from $V_{\text{max}} = 30\ \text{V}$ to zero. A positive domain of 400 nm length was formed. Another weak positive domain is also visible at the right end of the crystallite. The c -oriented BiT regions were also probed locally to check for the presence of ferroelectricity. Due to the very low piezoelectric constant along the c direction, the small oscillations induced could not be detected under the imaging conditions. However, a weak piezoelectric activity could be detected with the tip fixed over the matrix. Figure 10b shows the remanent hysteresis loop obtained in

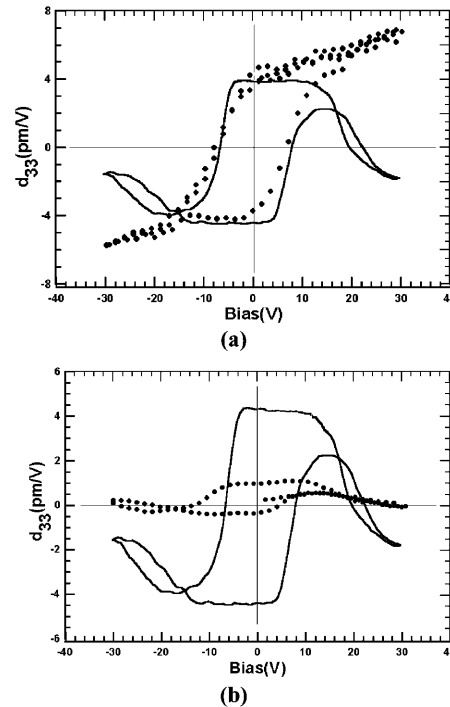


Fig. 10. **a** Remanent (—) and in-field (●) piezoelectric hysteresis loops of the grain shown in Fig. 9. **b** Remanent hysteresis loops of the grain (—) and of the c -oriented background (●)

the flat area, in comparison with the hysteresis loop of the grain. The ratio between the effective piezoelectric coefficient measured over the crystallite and that of the c -oriented region approximately amounts to 5. From the slope of the linear part of the in-field hysteresis loop, $\partial d/\partial U = (0.05 \pm 0.01)\text{pm}/\text{V}^2$ the electrostriction coefficient was calculated as $Q_c = (7.7 \pm 2) \times 10^{-3} \text{m}^4/\text{C}^2$. It is also possible to estimate the effective electrostriction coefficient for the crystallite, by using relation (2) written for the two cases and the known values for permittivities and spontaneous polarization from literature [25]. This simple estimation lead to a value of $Q_a = (1.47 \pm 0.5) \times 10^{-3} \text{m}^4/\text{C}^2$ for the effective electrostriction coefficient normal to the $(110)_{\text{orth}}$ plane.

3 Conclusions

The piezoresponse SFM technique was proven to be a powerful tool not only to image the ferroelectric domain structure, but also to characterize the ferroelectric thin films at the nanoscale. By using cantilevers that do not interact electrostatically with the bottom electrode it is possible to determine not only the local piezoelectric coefficient, but also the electrostriction coefficient and even the absolute polarization. It was proven that isolated grains of SBT having lateral sizes of 200 nm exhibit good ferroelectric behavior, showing a stable nano-domain structure. Also, ferroelectric domain structure, switching, and local characterization were achieved for BiT films for the first time.

It was experimentally shown that SBT, which is an even member of the Aurivillius family, exhibits ferroelectric behavior only in the ab plane, whereas BiT, being an odd member of the same family additionally exhibits a distinct piezoelectric hysteresis along the crystallographic c -direction.

Quantitative measurements at the nanoscale level, within the experimental errors give the same values for remanent polarization and coercive field as macroscopic ferroelectric measurements performed on the same samples.

References

1. J.F. Scott, M. Alexe, N.D. Zakharov, A. Pignolet, C. Curran, D. Hesse: *Integ. Ferroelec.* **21**, 1 (1998)
2. J. Lappalaianen, J. Frantti, V. Lantto: *J. Appl. Phys.* **82**, 3469 (1997)
3. E.C. Subarao: *J. Phys. Chem. Solids* **23**, 665 (1962)
4. O. Auciello, A. Gruverman, H. Tokumoto, S.A. Prakash, S. Aggarwal, R. Ramesh: *MRS Bulletin* **23**, 33 (1998)
5. P. G uthner, K. Dransfeld: *Appl. Phys. Lett.* **61**, 1137 (1992)
6. T. Hidaka, T. Maruyama, M. Saitoh, N. Mikoshiba, M. Shimizu, T. Shiosaki, L.A. Wills, R. Hiskes, S.A. Dicarolis, J. Amano: *Appl. Phys. Lett.* **68**, 2358 (1996)
7. A. Gruverman, O. Auciello, H. Tokumoto: *Appl. Phys. Lett.* **69**, 3191 (1996)
8. A. Gruverman, H. Tokumoto, S.A. Prakash, S. Aggarwal, B. Yang, M. Wuttig, R. Ramesh, O. Auciello, T. Venkatesan: *Appl. Phys. Lett.* **71**, 3492 (1997)
9. A. Gruverman, Y. Ikeda: *Jpn. J. Appl. Phys.* **37**, L939 (1998)
10. A. Gruverman, O. Auciello, H. Tokumoto: *Integ. Ferroelec.* **19**, 49 (1998)
11. D. Damjanovic: *Rep. Prog. Phys.* **61**, 1267 (1998)
12. G. Zavala, J.H. Fendler, S. Trolrier-McKinstry: *J. Appl. Phys.* **81**, 7480 (1997)
13. J.A. Christman, R.R. Woolcott Jr., A.I. Kingon, R.J. Nemanich: *Appl. Phys. Lett.* **73**, 3851 (1998)
14. A.L. Kholkin, E.L. Colla, A.K. Tagantsev, D.V. Taylor, N. Setter: *Appl. Phys. Lett.* **68**, 2577 (1996)
15. K. Franke: *Ferroelectr. Lett.* **19**, 35 (1995)
16. K. Franke, J. Besold, W. Haessler, C. Seegebarth: *Surf. Sci. Lett.* **302**, L283 (1994)
17. A. Pignolet, S. Welke, C. Curran, M. Alexe, S. Senz, D. Hesse: *Ferroelectrics* **202**, 285 (1997)
18. A. Pignolet, K.M. Satyalakshmi, M. Alexe, N.D. Zakharov, C. Harnagea, S. Senz, D. Hesse, U. G osele: *Integ. Ferroelec.* **26**, 21 (1999)
19. A. Pignolet, C. Sch afer, K.M. Satyalakshmi, C. Harnagea, D. Hesse, U. G osele: *Appl. Phys. A*, DOI 10.1007/s003390000177; **70**, 283 (2000)
20. A.L. Kholkin, K.G. Brooks, N. Setter: *Appl. Phys. Lett.* **71**, 2044 (1998)
21. S. Nomura, K. Uchino: *Ferroelectrics* **41**, 117 (1982)
22. A.L. Kholkin, M.L. Calazda, P. Ramos, J. Mendiola, N. Setter: *Appl. Phys. Lett.* **69**, 3602 (1996)
23. K. Franke, H. Huelz, M. Weihnacht: *Surf. Sci.* **416**, 59 (1998)
24. O. Auciello, J.F. Scott, R. Ramesh: *Phys. Today* **51**, 22 (1998)
25. Landolt-B ornstein: *Numerical Data and Functional Relationships in Science and Technology* Group III, Vol. 16, subvol. A, (Springer Berlin, Heidelberg, New York 1981) p. 237